

Article

Monitoring and Analysis of the Operation Performance of Vertical Centrifugal Variable Frequency Pump in Water Supply System

Jianyong Hu ^{1,2,*}, Chaohao Wang ³, Chengju Shan ^{2,4} and Yunhui Guo ^{1,2,5}

¹ School of Geomatics and Municipal Engineering, Zhejiang University of Water Resources and Electric Power, Hangzhou 310018, China; guoyh@zjweu.edu.cn

² Engineering Research Center of Digital Twin Basin of Zhejiang Province, Hangzhou 310018, China; shancj@zjweu.edu.cn

³ Guangdong Provincial Design Institute of Water Conservancy and Electric Power, Guangzhou 510635, China; wangch86@yeah.net

⁴ School of Water Conservancy and Environmental Engineering, Zhejiang University of Water Resources and Electric Power, Hangzhou 310018, China

⁵ School of Electric Power, North China University of Water Resources and Electric Power, Zhengzhou 450045, China

* Correspondence: hujy@zjweu.edu.cn

Abstract: The stable operation of a variable frequency pump is of great importance to the management of a water supply project. Analyzing the operation performance based on monitoring data is necessary for maintaining the stable operation of a variable frequency pump. Several sensors are installed at six monitoring points on the pump to collect signals including vibration velocity, vibration acceleration and vibration displacement. Monitoring signals are preprocessed by smoothing, adjusting waveform trend and filtering on the basis of Fast Fourier Transform (FFT). Then, the vibration features are extracted by power spectrum analysis and cepstrum analysis methods. According to the extracted features, the vibration law and actual operation performance of a variable frequency pump under different operating conditions are analyzed. Results indicate that the vibration amplitude of the pump varies sharply under the operating conditions of [15 Hz, 20 Hz] and [30 Hz, 35 Hz]. The operating condition of [0 Hz, 15 Hz] is the restricted operating area of the pump. The vibration and noise continue increasing under the operating conditions of [35 Hz, 50 Hz] and reach the maximum values at 50 Hz. Therefore, the optimal operating is within the range of [20 Hz, 30 Hz]. Finally, by analyzing the critical values of the operating conditions, the fault diagnosis and the evaluation of the operating status are conducted.

Keywords: variable frequency pump; vibration signal; spectrum analysis; Fourier transform; operation performance analysis



Citation: Hu, J.; Wang, C.; Shan, C.; Guo, Y. Monitoring and Analysis of the Operation Performance of the Operation Performance of Vertical Centrifugal Variable Frequency Pump in Water Supply System. *Energies* **2023**, *16*, 4526. <https://doi.org/10.3390/en16114526>

Academic Editor: Helena M. Ramos

Received: 17 April 2023

Revised: 29 May 2023

Accepted: 2 June 2023

Published: 5 June 2023



Copyright: © 2023 by the authors. Licensee MDPI, Basel, Switzerland. This article is an open access article distributed under the terms and conditions of the Creative Commons Attribution (CC BY) license (<https://creativecommons.org/licenses/by/4.0/>).

1. Introduction

The performance monitoring of a variable frequency pump in a water supply system is to collect the vibration signal at monitoring points by setting sensors and extracting relevant parameters. Generally, a vibration signal can be extracted in the time domain, the amplitude domain and the frequency domain. The Fast Fourier Transform (FFT) method is effective in spectrum refinement calculation and analysis [1–3]. Most monitoring signals are nonstationary signals containing lots of noise. Vibration signals with cluttered noise can be processed using the FFT method. Wavelet packet signal processing and a decision tree algorithm can be used to reduce the interference of noise in vibration signals and extract features for fault diagnosis. Analyzing the noise signal and other signals measured from multiple sensors can evaluate the running performance of the pump system [4–6]. In order to improve the instantaneous frequency identification accuracy of nonstationary signals, the

improved synchronous extrusion wavelet transform method has been used to preprocess nonstationary signals [7]. In the vibration signal analysis of hydropower units, the method based on an adaptive local iteration filter can be used to improve the efficiency and accuracy of feature extraction of nonstationary vibration signals [8]. For the time frequency analysis, the Vold–Kalman filter can be used to extract frequency components, then time–frequency analysis (TFR) of each single channel component can be conducted using the time-frequency post-processing method. The TFR of an original signal is constructed by superposition to realize TFR with high time-frequency resolution [9]. The original mixed clutter features can also be extracted in the time domain, the frequency domain and the time-frequency domain. The correlation coefficients can be estimated from the correlation sequences generated by the intersection of health signals and vibration signals to extract the vibration features and improve the accuracy of fault diagnosis of the pump [10]. At present, the time-frequency domain analysis of vibration signals is the main method for fault diagnosis.

There are two commonly used methods for evaluating the performance of a pump: one is vibration signal frequency analysis; the other is multiple influence factor analysis. The health assessment model of a pump can be established based on the relation mapping between the vibration data and operation performance, with which the future performance can be predicted [11]. To analyze the features of vibration signals for fault diagnosis, a high-precision fault diagnosis model was proposed to extract features by combining the vibration extremum, binary wavelet energy time spectrum and coefficient power spectrum [12]. In addition, based on the adaptive neurofuzzy inference system, an intelligent diagnosis system was developed, where the vibration signal features can be extracted under the conditions of looseness and misadjustment [13]. A combination of symbolic perception points and hidden Markov models has also been used in the fault diagnosis of a pump, which has a good performance under poor information conditions [14]. With the development of computer techniques, online fault monitoring of a pump has been developed, the variation laws of pump operation parameters have been evaluated using artificial neural network algorithms, and pump performance can be evaluated from the time–frequency distribution analysis and spectrum analysis [15–17]. The fault diagnosis is conducted based on the fault database and intelligent diagnosis algorithm, which is finally realized through an online diagnosis system [18]. The commonly used intelligent algorithms for fault diagnosis of a pump include neural network method, fuzzy diagnosis, support vector machine method and fault tree analysis. Combining the test ability-oriented fault mode and T-FMEA diagnostic requirements, the neural network method can be used to diagnose faults in a pump and extract fault-related features from the instantaneous power spectrum [19,20]. As the monitoring signals are usually incomplete and the state identification are usually inaccurate, research on the comprehensive performance evaluation of pumps based on monitoring data is not sufficient. In addition, the selection of the main characteristics is not unified when the spectrum analysis and feature extraction are processed.

Wavelet methods are also widely used in signal analysis. Wavelet transformation is a local transformation of space–time and frequency, which can effectively extract features from signals. The multiscale detailed analysis of signals can be promoted through operation functions such as scaling and translation, which solves many difficult problems that cannot be solved by the Fourier transform. The combination of neural network methods and wavelet analysis is one of the research hotspots. A noise signal analysis method based on incomplete wavelet packet analysis and an artificial neural network has been presented, which is effective in the feature extraction of engine fault noises in both time and frequency domains and is powerful in sound feature classification and faults recognition [21]. Motivated by deep learning theory, an intelligent fault diagnosis method combining wavelet analysis and the improved convolution neural network (CNN) method has been used to improve the accuracy of the calculation. Compared with the classic Alex-Net, the proposed method decreases the number of parameters and reduces the computational complexity by modifying the structure of the network. The model integrates the advantage of wavelet

analysis in feature extraction and method in deep learning. It not only has high recognition accuracy but also is robust [22]. In order to improve the denoising ability of wavelet analysis, optimal wavelet multiresolution analysis has been employed for reducing noise from vibration signals and interference of noise in monitoring signals. The enhanced independent component analysis algorithm overcomes the shortcomings of the ICA algorithm and allows the selection of reliable independent components; it has been adopted for source separation spectra analysis. This method can efficiently be employed to both isolated and combined mechanical faults diagnosis [23]. An attempt was conducted for hydraulic pump faults diagnosis based on modified empirical mode decomposition, auto regressive spectrum and nuclear wavelet limit learning machine methods [24]. Additionally, the use of wavelet packet analysis technology can overcome the disadvantage of poor resolution of traditional wavelet analysis and provide an accurate signal decomposition method [25].

At present, in the field of pump fault diagnosis, a number of theoretical methods have been proposed and applied. However, the operating conditions of variable-frequency pumps are complex due to their large adjustable range and the difficulty of feature extraction. The research on the fault diagnosis of variable-frequency pumps is still lacking. Analyzing the real-time operation data is still one of the main methods for the fault diagnosis of variable-frequency pumps [26]. Recently, multi-sensor monitoring has been widely used to identify pump fault modes, which combines acoustic emission signals and vibration acceleration signals [27]. In the test, multitype sensors can be used to collect multitype signals and analyze the operation performance of the pump.

The key point of fault diagnosis of variable-frequency pumps is to analyze the features of vibration signals and estimate the variation in operation performance through monitoring data. In this study, we installed several different types of sensors at six monitoring points on the pump to collect signals including vibration velocity, vibration acceleration and vibration displacement. Monitoring signals are preprocessed using signal smoothing, waveform trend adjustment and filtering on the basis of Fast Fourier Transform (FFT). We then extract the vibration features with power spectrum analysis and cepstrum analysis and estimate the energy features using wavelet transformation. The flowchart of the test is shown in Figure 1.

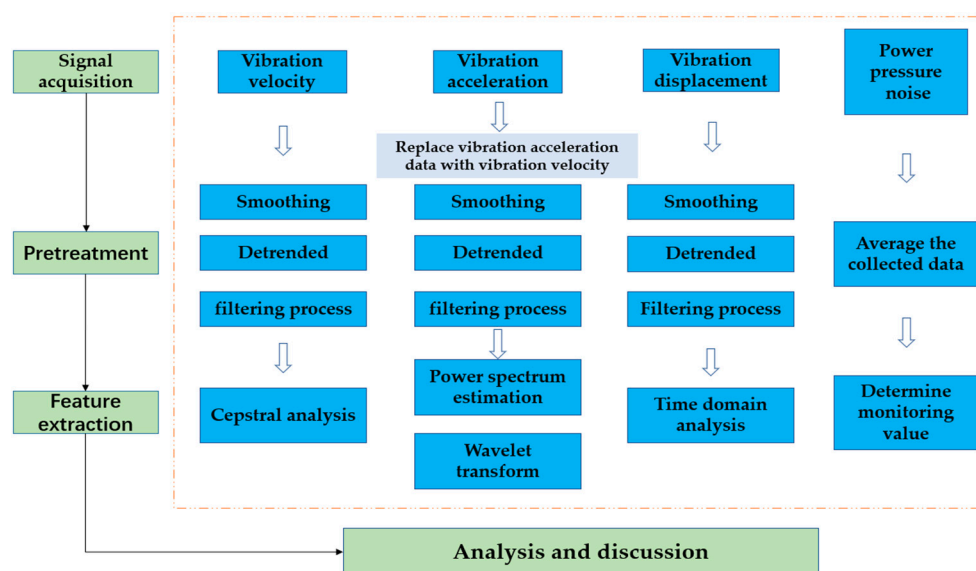


Figure 1. The flowchart of the test.

In Section 2, the test platform used in this research is introduced and signal acquisition under different test conditions is carried out by arranging sensors. In Section 3, the methods of preprocessing and feature extraction are introduced and signal preprocessing is conducted via smoothing, waveform trend adjustment and filtering, and spectrum feature extraction is conducted via power spectrum estimation and cepstrum analysis. In Section 4,

by processing and analyzing the vibration signals, pressure and noise signals, the operation performance of the variable-frequency pump is analyzed. In Section 5, the conclusions are summarized. This study provides a reference for improving the operation performance of variable-frequency pumps based on monitoring data.

2. Tests and Data

2.1. Test Platform

This study was conducted based on a physical model test system. Figure 2a,b show the panoramagram and close-range diagram of the test platform, respectively. The model is equipped with a three-stage booster pump station. The first-stage booster pump station is equipped with three pumps which are in parallel with each other. Among which, the first station is a large vertical centrifugal variable-frequency pump; the second and third stations are equipped with normal pumps. In this research, the vertical centrifugal variable-frequency pump of the first station was selected as the research object.



Figure 2. Test platform of the pipeline water conveyance: (a) panoramagram, (b) close-range diagram.

2.2. Monitoring Point Layout

According to the design scheme and structural characteristics of the variable-frequency pump, the parameters of the pump are shown in Table 1. In the physical model test, eight operating conditions, namely 15 Hz, 20 Hz, 25 Hz, 30 Hz, 35 Hz, 40 Hz, 45 Hz and 50 Hz, were selected as the high-frequency operating area of the pump. In the performance monitoring analysis, vibration signal analysis is the main analyzing method. Power, pressure and noise signal analyses are auxiliary methods. The layout of the monitoring points is shown in Figure 3. The monitoring points and sensor types as shown in Table 2.

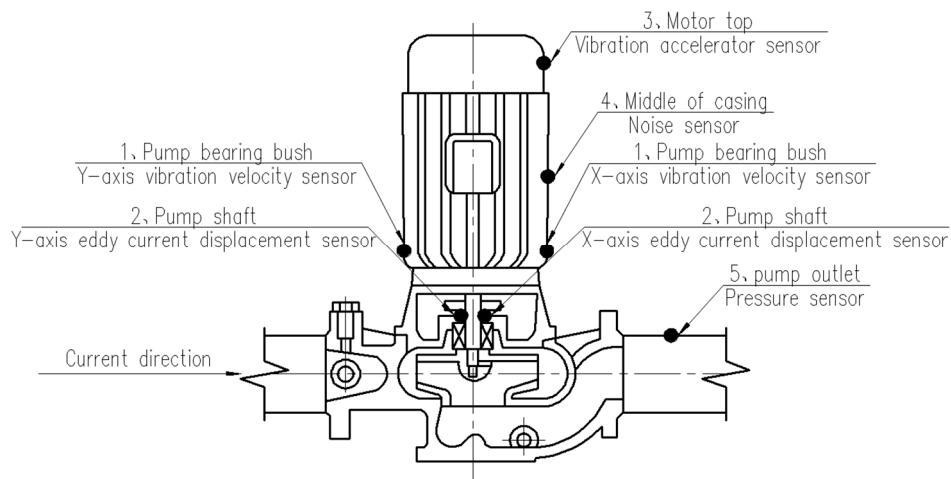


Figure 3. Layout of the monitoring points.

Table 1. Main parameters of the vertical variable frequency pump.

Electric Motor (YE2-160M1-2)					Pump				
Rated Power (kW)	Rotation Rate (r/min)	Efficiency (%)	Power Factor	Rated Torque (N/m)	Noise (dB)	Weight (kg)	Design Flow (m ³ /h)	Rated Speed (r/min)	Head (m)
11	2930	88.4	0.89	35.9	86	103	100	2900	20

Table 2. Selection of monitoring points and sensor types in the vibration evaluation of pump components.

Monitoring Point Location	Parameter	Sensor Type	Range
Pump bearing bush	Vibration velocity (mm/s)	Vibration velocity sensor	Measuring range 0–30 (mm/s)
Pump shaft	Vibration displacement (mm)	Eddy current displacement sensor	Frequency response Range 0–5000 (Hz)
Motor top	Vibration acceleration (mm ² /s)	Vibration acceleration sensor	Range of working temperature 54–121 (°C)
Middle of casing	decibel (dB)	Noise sensor	Measured value 30–130 (dB)
Pump outlet	decibel (Pa)	Pressure sensor	Range 0–1.6 (Mpa)
Three-phase connection of motor	power (W)	Power sensor	Input frequency 40–75 (Hz)

3. Method

For processing the signals collected by the sensors, we first used the Fast Fourier Transform (FFT) method to realize the time–frequency domain transformation, so as to reduce the number of calculations in the signal preprocessing. In the Fourier transform, the Hamming window function is used for signal interception:

$$\omega(t) \begin{cases} 0.54 + 0.46\cos\left(\frac{\pi t}{T}\right), 0 < t < T \\ 0, t \notin (0, T) \end{cases} \quad (1)$$

where t is time and T is the period.

3.1. Signal Pre-Processing

When the pump fails, the vibration signal is a nonstationary signal, mixed with high-frequency noise. Therefore, preprocessing should be performed for monitoring signals before the feature extraction. In this paper, the preprocessing of signals was carried out using smoothing, waveform trend adjustment and filtering.

The smoothing method has a good performance in processing waveform burrs in vibration signals and eliminating high-frequency noise. This paper adopts the five-point moving average method ($N = 2$) to smooth the signals:

$$\left. \begin{aligned} y_1 &= \frac{1}{5}(3x_1 + 2x_2 + x_3 - x_4) \\ y_2 &= \frac{1}{10}(4x_1 + 3x_2 + 2x_3 + x_4) \\ &\vdots \\ y_i &= \frac{1}{5}(x_{i-2} + x_{i-1} + x_i + x_{i+1} + x_{i+2}) \\ &\vdots \\ y_{m-1} &= \frac{1}{10}(x_{m-3} + 2x_{m-2} + 3x_{m-1} + 4x_m) \\ y_m &= \frac{1}{5}(-x_{m-3} + x_{m-2} + 2x_{m-1} + 3x_m) \end{aligned} \right\} (i = 3, 4, \dots, m-2) \quad (2)$$

where x is the sampling data; y is the corresponding calculation result; m is the number of data points. Compared with other filtering methods, the advantage of the five-point method is its high stability and adaptability. It takes the average of data at several time points, which greatly reduces the effect of random error and can be applied to deal with most types of vibration signals. In addition, as the five-point method does not have to set the filter parameters, the calculation process is relatively simple, and the calculation speed is fast.

The signal data collected by the sensor are discrete, and their vibration trend deviates from the baseline; the deviation varies with time, causing the overall waveform to deviate from the baseline. The method for adjusting the waveform trend is the polynomial least squares method, which can eliminate the trend item to adjust the waveform.

In filtering, a digital filter was used to eliminate and weaken discrete noise, and to extract signals that can reflect the operating status of the pump. According to the maximum vibration frequency of the test object within 300 Hz, a low-pass Chebyshev type I filter was selected to extract useful signals. The low-pass Chebyshev type I filter not only has a good performance in noise reduction but also has high adaptability to deal with vibration signals. In addition, its low order characteristic greatly reduces the calculation.

3.2. Signal Feature Extraction

The feature extraction of signals is a process of frequency-domain conversion using corresponding algorithms based on the preprocessed time-domain signal. In this paper, power spectrum analysis method and cepstrum analysis method are used to extract the features.

The power spectrum estimation method characterizes monitoring signals with calculation statistics. The random signal spectrum function is segmented using the average period method. After adding the window function, each segment of the signal is subjected to a fast Fourier transform, and finally the power spectral density is calculated. On the basis of the average time method of the random vibration function, the self-power spectral density function is presented in Formula (3).

$$S_{xx}(k) = \frac{1}{MN_{FFT}} \sum_{i=1}^M X_i(k) X_i^*(k) \quad (3)$$

where $X_i(k)$ is the Fourier transform of the i -th data segment; $X_i^*(k)$ is the conjugate complex number of $X_i(k)$; N is the number of sample data; M is the average number of times.

The cepstrum analysis method can simplify the chaotic periodic components in the spectrum diagram and visually represent the vibration under different frequency doublings. The convolution relationship in the original signal can be converted into an additive relationship in logarithmic form to eliminate the unnecessary components in the monitoring signal and obtain data reflecting the operation performance of the pump. The expressions are shown in Formulas (4) and (5).

$$C_p(q) = |F\{\lg G_x(f)\}|^2 \quad (4)$$

$$C_p(q) = \sqrt{C_p(q)} = |F\{\lg G_x(f)\}| \quad (5)$$

where q is the reciprocal frequency and f is the frequency.

4. Results and Analysis

4.1. Vibration Velocity Spectrum Extraction

The vibration velocity sensor was installed on the x and y axes of the pump bearing bush to collect signals of vibration velocity. Through the cepstrum feature extraction, the vibration of the pump foundation, support and pump impeller during the operation of the pump was monitored. Through the vibration value, the fault characteristics such as loose foundation bolts, loose fixing between the driving device frame and the foundation, impeller mass deviation and friction between the impeller and pump body were analyzed. In the feature extraction, the Fourier transform is used for the time–frequency domain transformation, and the number of sampling points should be a power of two. An insufficient number of sampling points cannot fully reflect the operating features of the pump, and an excessive number of sampling points will lead to cumbersome calculation steps. The frequency of the variable frequency pump can be adjusted within the range of 0 Hz to 50 Hz. The frequency of the vibration signals is one to five times the frequency of the

pump, that is, the frequency of the vibration signal reaches the maximum value of 250 Hz under the working condition of 50 Hz. Therefore, to avoid signal interference and reduce computing time, we only consider vibration signals under 300 Hz. Therefore, the sampling point frequency was 1024 Hz and the time interval was 976 μ s. The adopted point length was 1024.

The cepstrum analysis results of vibration velocity signals under the test conditions of 15 Hz, 25 Hz, 35 Hz and 45 Hz at the indicated monitoring points are shown in Figure 3. The vibration velocities in the x-axis direction and the y-axis direction are obtained from the spectrum analysis under different operating conditions. The peak values of the vibration velocities both in the x-axis direction and the y-axis direction increase with the increasing frequency of the pump. Under the working condition of 15 Hz, the maximum peak values of the vibration velocity ranges in the x-axis direction and the y-axis direction are 0.41 mm/s and 0.32 mm/s, respectively. Under the working condition of 45 Hz, the maximum peak values of the vibration velocity ranges in the x-axis direction and the y-axis direction reach 2.02 mm/s and 2.19 mm/s, respectively.

Since the spectrum diagram can only reflect the vibration trend and the overall operation performance of the pump, it is necessary to analyze the vibration speed of the pump under different working conditions. The arrangement of the vibration values of the monitoring points is shown in Table 3. By comparing the data in Table 3, the vibration range can be determined. The maximum vibration difference under the operating conditions of [15 Hz, 30 Hz] in the x-axis was 0.45 mm/s. Under the operating conditions of [30 Hz, 35 Hz], the maximum vibration difference between adjacent operating conditions increased, and the maximum vibration difference under the operating conditions of [30 Hz, 35 Hz] reached 1 mm/s. Under the conditions of [40 Hz, 50 Hz], the vibration value was about 2 mm/s. In the y-axis direction, the variation trend of the vibration value was basically consistent with the x-axis direction. Under the working condition of 25 Hz, the transfer of vibrational energy increases the quadruple frequency. Under the working condition of [45 Hz, 50 Hz], the pump works under its maximum rotational speed, and the rate of the input flow also reaches its maximum. In this case, the running status of the pump reaches the upper limit, and the nonlinear vibration occurs in the pump which leads to a significant increase in quintuple frequency.

Table 3. Vibration of the measuring points under different test conditions.

Test Conditions	Frequency Doubling (mm/s)	Double Frequency (mm/s)	Triple Frequency (mm/s)	Quadruple Frequency (mm/s)	Quintuple Frequency (mm/s)	Maximum Vibration Effective Value (mm/s)
15 Hz (X)	0.4087	0.1829	0.2564	0.1050	0.1842	0.4087
15 Hz (Y)	0.3243	0.1679	0.2506	0.2199	0.0670	0.3243
20 Hz (X)	0.5143	0.0913	0.1003	0.0227	0.0235	0.5143
20 Hz (Y)	0.5278	0.2077	0.3119	0.0715	0.0402	0.5278
25 Hz (X)	0.1724	0.2991	0.4325	0.4624	0.3481	0.4624
25 Hz (Y)	0.1031	0.2112	0.1125	0.3142	0.0233	0.3142
30 Hz (X)	0.9394	0.3874	0.5212	0.3185	0.1617	0.9394
30 Hz (Y)	0.8652	0.3133	0.4170	0.5283	0.1988	0.8652
35 Hz (X)	1.9527	0.2373	0.2066	0.1612	0.6447	1.9527
35 Hz (Y)	1.6080	0.2811	0.2931	0.2132	0.0564	1.6080
40 Hz (X)	2.0210	0.5020	1.3636	0.1575	0.0594	2.0210
40 Hz (Y)	2.2499	0.4157	0.8953	0.2331	1.8312	2.2499
45 Hz (X)	0.1623	0.5102	0.9573	0.8146	2.0220	2.0220
45 Hz (Y)	0.2175	0.5459	1.0805	0.6754	2.1901	2.1901
50 Hz (X)	0.1607	0.6064	1.3801	1.8641	1.9420	1.9420
50 Hz (Y)	0.7717	0.5200	0.8475	1.7938	2.7514	2.7514

4.2. Vibration Acceleration Spectrum Extraction

A vibration acceleration sensor was installed at the top of the motor to collect the vibration acceleration data. In this model test, to estimate whether the operation performance of the pump is abnormal, the vibration acceleration signal was calculated, and the features of the pump were extracted. The vibration range of the pump is [0 Hz, 300 Hz]; this range does not belong to the high-frequency range. While the acceleration signal is usually suitable for high-frequency signal analysis, the vibration velocity signal is more suitable for medium-frequency signal analysis. In order to ensure the accuracy of the analysis, the vibration acceleration signal was converted into vibration velocity data before processing.

The spectrum processing results of the vibration signal at the monitoring point at the top of the motor under different working conditions are shown in Figure 4. According to the spectrum analysis under different operating conditions, the variation trend of the vibration under different operating conditions was analyzed. The vibration value was too high at 15 Hz, while it was generally stable under the operating conditions of [20 Hz, 35 Hz]. The vibration became larger at 40 Hz, and the value further increased under the operating conditions of [45 Hz, 50 Hz]. The analysis showed that the vibration difference of the pump was large between 15 Hz and 20 Hz, and there was a critical operating condition that caused a sudden change in the pump operation performance within this range. Under the operating conditions of [40 Hz, 50 Hz], the vibration range became large and reached the maximum value.

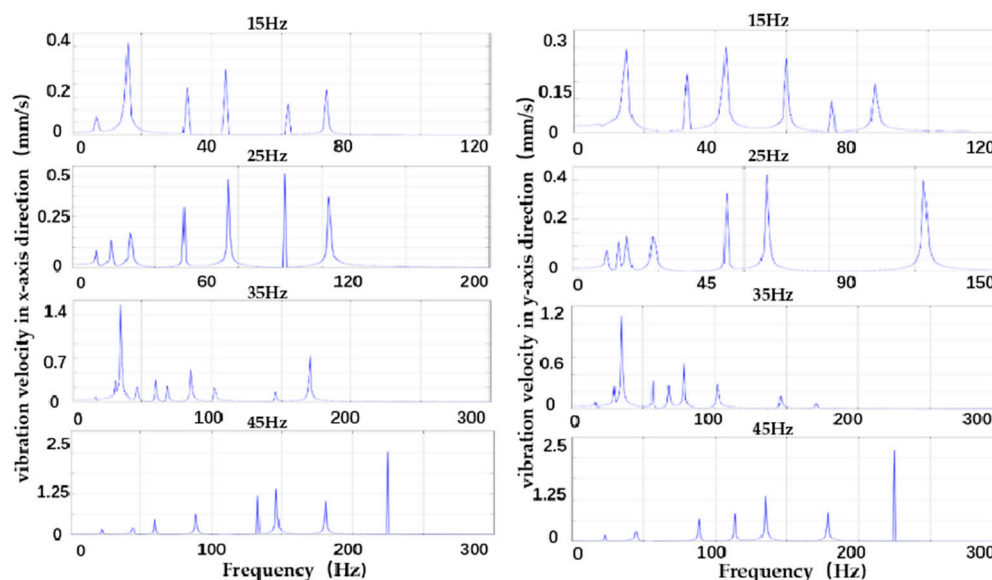


Figure 4. Cepstrum analysis of vibration velocity signal in x and y direction.

Since the spectrum diagram only reflects the vibration change trend, the specific vibration value was compared with the vibration speed of different frequency doubling under the same operating conditions. The motor vibration values under different frequency doubling are shown in Table 4. The revolution speed under 15 Hz, 20 Hz, 25 Hz, 30 Hz, 35 Hz, 40 Hz, 45 Hz and 50 Hz are 892.75 r/min, 1201.33 r/min, 1489.25 r/min, 1781.25 r/min, 2086.33 r/min, 2387.75 r/min, 2610 r/min and 2966 r/min, respectively. According to the comparison of different frequencies of the pump under different operating conditions, it can be seen that the vibration value at 15 Hz was larger than that at 20 Hz, being 1.1 mm/s larger in the x-axis direction, 2.4 mm/s larger in the y-axis direction and 4.2 mm/s larger in the z-axis direction. When the pump was operating under the conditions of [20 Hz, 30 Hz], the vibration value of the monitoring point at the top of the motor did not change significantly. The overall vibration value was small, but the value at 35 Hz was larger than that at 30 Hz, in which the quintuple frequencies in the x-axis and z-axis directions were 1.8 mm/s larger, and the primary frequencies in the x-axis, y-axis and z-axis directions were about

81 mm/s larger. When the pump was operating above 40 Hz, the maximum vibration value occurred.

Table 4. Motor vibration values under different test conditions.

Test Conditions	Revolution Speed (r/min)	Frequency Doubling (mm/s)	Double Frequency (mm/s)	Triple Frequency (mm/s)	Quadruple Frequency (mm/s)	Quintuple Frequency (mm/s)
15 Hz (X)		1.6379	0.0392	0.0329	0.0326	0.2981
15 Hz (Y)	892.75	3.7638	0.0409	0.1333	0.0103	1.6901
15 Hz (Z)		5.4404	0.0192	0.0102	0.0243	0.2228
20 Hz (X)		0.5506	0.2547	0.1148	0.1207	0.0742
20 Hz (Y)	1201.33	1.3903	0.1410	0.8357	0.4960	0.1930
20 Hz (Z)		1.2204	0.0380	0.1301	0.1477	0.0485
25 Hz (X)	1489.25	0.7117	0.3125	0.2945	0.0224	0.2223
25 Hz (Y)		0.6545	0.1476	0.3928	0.0642	0.1292
25 Hz (Z)		0.9940	0.0675	0.1943	0.0843	0.2974
30 Hz (X)	1781.25	1.7723	0.9567	0.5382	0.0365	0.9598
30 Hz (Y)		1.1970	0.1580	0.1498	0.0354	1.9438
30 Hz (Z)		1.2505	0.0479	0.3250	0.0729	0.7077
35 Hz (X)	2086.33	2.1788	1.8347	0.4084	0.4451	2.7167
35 Hz (Y)		1.9897	0.5806	0.5899	0.2527	1.6424
35 Hz (Z)		1.9240	1.8458	0.1742	0.0740	0.5031
40 Hz (X)	2387.75	5.1037	2.2299	0.5735	1.5150	6.4349
40 Hz (Y)		3.5834	2.8341	0.0868	0.3548	0.3112
40 Hz (Z)		3.1881	2.1025	0.2373	0.5989	5.5656
45 Hz (X)	2610.00	1.7898	2.3343	0.3803	4.2980	12.1483
45 Hz (Y)		4.8144	5.8025	0.4873	1.0763	1.5199
45 Hz (Z)		3.4333	3.5153	0.3446	1.9837	6.9741
50 Hz (X)	2966.00	5.2483	1.5788	0.4401	9.4100	11.4539
50 Hz (Y)		13.8825	1.7218	1.0986	3.2779	5.6900
50 Hz (Z)		6.1320	1.3250	0.9894	12.3624	1.4108

To sum up, according to the comparative analysis of the vibration value of the monitoring point at the top of the motor, the pump had critical points that caused a sudden change in the operating performance under the operating conditions of [15 Hz, 20 Hz] and [30 Hz, 35 Hz]. Additionally, the vibration reached its maximum value under the working condition of [40 Hz, 50 Hz].

4.3. Characteristic Analysis of Vibration Displacement Signal

For the rotating shaft of the vertical centrifugal variable-frequency pump, an eddy current displacement sensor was installed along the horizontal and vertical directions, and the operation performance was analyzed by collecting the vibration displacement signals. Because the rotating frequency of the rotating shaft of the variable-frequency pump is usually adjusted by the governor, the other frequency-doubled vibrations are not obvious, and the eddy current displacement sensor is affected by the metal parts around the rotating shaft, where the collected vibration displacement signal is mixed with interfering signals. Therefore, time-domain analysis was carried out after the preprocessing. The operating performance of the rotating shaft of the pump under different test conditions is reflected through the statistics of the data. Figure 5 shows the time-domain diagram of the collected raw vibration and displacement signal data of the rotation axis measurement point after processing. According to the analysis of the time-domain diagrams under the test conditions of 15 Hz, 25 Hz, 35 Hz and 45 Hz (Figure 6), the vibration displacement balance position in the x-axis direction of the pump was concentrated at about 0.05 mm, while in the y-axis direction, it was concentrated at about −0.15 mm. There was a slight swing when the pump was operated under different operating conditions.

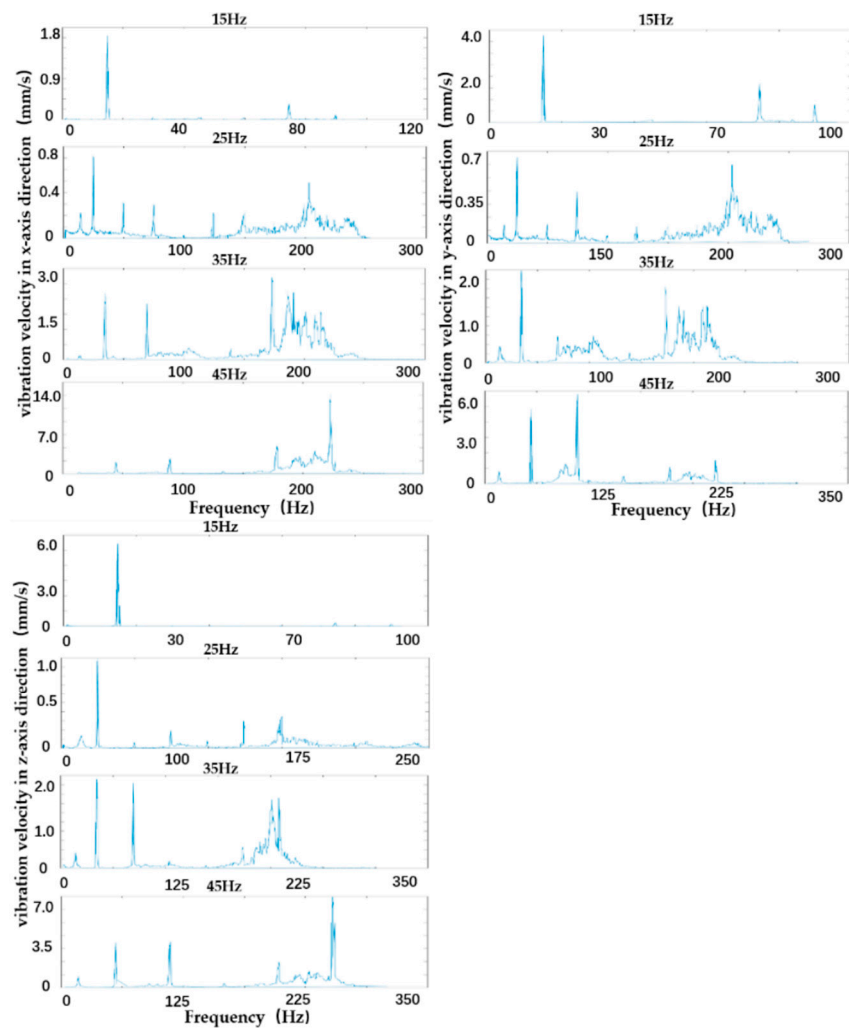


Figure 5. Spectrum analysis of vibration signal of measuring point at the top of motor.

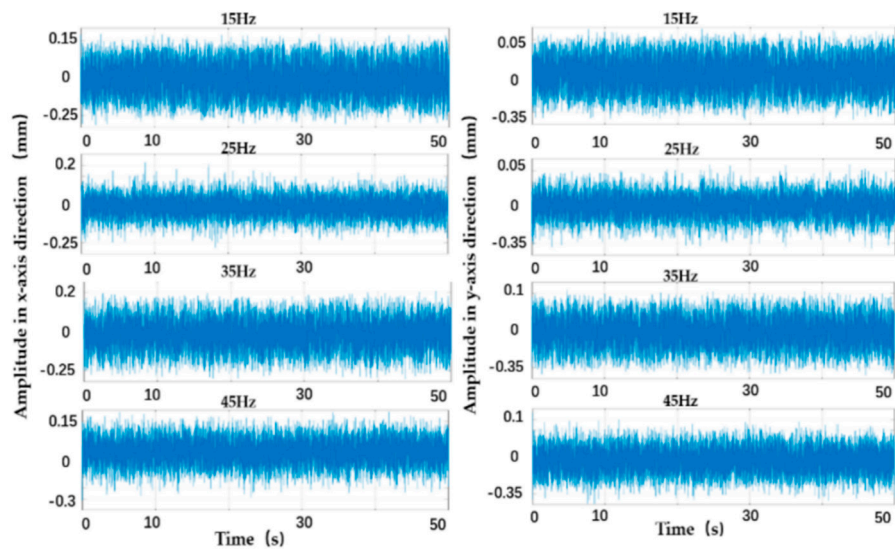


Figure 6. Time domain diagram of vibration displacement signal under different test conditions.

In order to clarify the vibration range of the rotating shaft of the pump under different test conditions, the statistical characteristics of the pretreated x-axis and y-axis vibration displacement directions were analyzed at four statistics, namely, the mean value, variance,

range and main vibration range were selected for calculation and comparison. The mean value reflects the static part of the signal, and it is used to represent the balance position of the vibration. The variance reflects the dynamic part of the signal, indicating the amplitude variation range of the vibration signal centered on the equilibrium position. The range reflects the maximum vibration range of the signal. The main vibration range excludes interference signals and high-frequency signals. The statistical results of each operating condition are shown in Table 5. It can be seen that the vibration value in the x-axis of the rotating shaft was the largest under the operating condition of 15 Hz. Under the working condition of 20 Hz, the vibration value decreased, and it was basically the same between [20 Hz and 45 Hz] and stable at about -0.037 mm/s. When the pump was operating at 50 Hz, the vibration became larger. When the pump operates under [15 Hz, 35 Hz], the square difference was the largest, that is, the fluctuation of the vibration under these two conditions was the largest. The fluctuation at [20 Hz and 30 Hz] was basically the same. The vibration fluctuation was not significant in the range of [15 Hz, 40 Hz], and the vibration fluctuation difference at [40 Hz and 50 Hz] was large, indicating that the vibration range of the rotating shaft was the largest at [40 Hz and 50 Hz].

Table 5. Shaft vibration displacement signal statistics.

Test Conditions	Spindle Speed (r/min)	Average Value (mm)	Variance (mm ²)	Range (mm)	Main Vibration Range (mm)
15 Hz (X)	892.75	-0.05371	0.00430	0.3642	[0.01, -0.12]
15 Hz (Y)		-0.14350	0.00450	0.3743	[-0.08, -0.21]
20 Hz (X)	1201.33	-0.03581	0.00260	0.3423	[0.01, -0.09]
20 Hz (Y)		-0.14450	0.00280	0.3608	[-0.09, -0.20]
25 Hz (X)	1489.25	-0.03797	0.00190	0.3829	[0.01, -0.08]
25 Hz (Y)		-0.14550	0.00200	0.3469	[-0.10, -0.19]
30 Hz (X)	1781.25	-0.03801	0.00320	0.3650	[0.02, -0.09]
30 Hz (Y)		-0.13160	0.00320	0.3835	[-0.07, -0.19]
35 Hz (X)	2086.33	-0.03774	0.00410	0.3981	[0.03, -0.10]
35 Hz (Y)		-0.13140	0.00440	0.3976	[-0.07, -0.20]
40 Hz (X)	2387.75	-0.03722	0.00360	0.4112	[0.02, -0.10]
40 Hz (Y)		-0.13900	0.00370	0.3986	[-0.08, -0.20]
45 Hz (X)	2610.00	-0.03847	0.00300	0.3982	[0.02, -0.09]
45 Hz (Y)		-0.14320	0.00313	0.4305	[-0.09, -0.20]
50 Hz (X)	2966.00	-0.04380	0.00320	0.3827	[0.01, -0.10]
50 Hz (Y)		-0.14470	0.00330	0.3985	[-0.09, -0.20]

The analysis shows that the vibration range of the pump under the operating conditions of [20 Hz, 50 Hz] was basically the same, and the vibration range at 15 Hz was larger than that under other conditions. Therefore, there was a critical point within the operating ranges of [15 Hz, 20 Hz] and [30 Hz, 35 Hz].

4.4. Characteristic Analysis of Power, Pressure and Noise Signals

The data were collected by installing a power sensor near the wiring of the motor, a noise sensor in the middle of the casing and a pressure sensor at the outlet of the pump. The data are shown in Tables 6–8. The measured data were averaged to determine the monitoring values under different operating conditions, and to analyze the change trend of the operation performance of the pump.

Table 6. Comparison of the motor power.

Test Conditions(Hz)	15	20	25	30	35	40	45	50
Motor Power (kW)	0.18	0.33	0.53	0.85	1.21	1.71	2.31	3.05

Table 7. Comparison of outlet pressure of pump.

Test Conditions(Hz)	15	20	25	30	35	40	45	50
Pressure (pa)	16,942	37,344	42,017	36,963	40,825	62,964	56,079	73,804

Table 8. Comparison of noise of pump.

Test Conditions (Hz)	15	20	25	30	35	40	45	50
Noise (dB)	72.61	76.62	79.52	83.35	84.94	90.92	90.89	94.31

The motor power increased with the increase in frequency. However, the rated motor power was significantly different from the measured value, resulting in the low-efficiency operation of the pump. The reason is that the water level of the tank cannot satisfy the water pressure required for the operation of the pump, and the loss along the way increases during water supply. However, the initial conditions of the model test were the same as those of each test condition, so the measured values can still generally reflect the changes in the operation performance of the pump.

As shown in Table 7, the minimum pressure of the pump was observed under the working condition of 15 Hz, and the maximum pressure was observed under the working condition of 50 Hz. The general tendency is that the pressure increases with the increased the frequency. However, some fluctuations should be noticed, for instance, the pressure at 25 Hz was higher than those at 20 Hz and 30 Hz, the pressure at 40 Hz was higher than those at 35 Hz and 50 Hz.

As can be seen from the noise of the pump in Table 8, the value increased with the increase in the operation frequency. According to the calibrated noise value, taking 86 dB as the boundary of the analysis, the noise in the operating condition range of [40 Hz, 50 Hz] exceeded the calibrated value, indicating that the pump had a large vibration in this range.

In short, the power of the pump under each operating condition was greatly different from the rated motor power, and the overall pump operation performance deviated from the theoretical characteristic curve. The variation in the pump outlet pressure was basically consistent with the results of the vibration signal analysis according to the spectrum and statistics, so the accuracy of the critical point was verified. According to the comparison between the noise value and calibrated value, the noise value of the pump exceeded the standard value under the operating conditions of [40 Hz, 50 Hz], indicating that the friction of the mechanical parts became larger and the operation performance of the pump was poor.

5. Fault Diagnosis of the Vertical Centrifugal Variable Frequency Pump

5.1. Determination of the Range of Critical Operating Conditions

Table 9 shows the range of critical operating conditions determined from vibrations at different positions. As can be seen from Table 9, there are two critical operating conditions: one is located within the range of [15 Hz, 20 Hz]; the other is located within the range of [30 Hz, 35 Hz]. According to the median approximation method, we analyzed the vibration data at the operating conditions of 18 Hz and 33 Hz, respectively. Spectrum analysis is conducted for the vibration signals of the monitoring point at the top of the motor. Wavelet transform analysis is conducted for the shaft vibration signals.

Figure 7 shows the spectrum diagram of the vibration signals of the monitoring point at the top of the motor under the working conditions of 18 Hz in (a) X, (b) Y and (c) Z directions. Under the working condition of 18 Hz, the vibration of the frequency doubling area at the top measuring point of the motor is the smallest in the y-axis, and the difference in vibration between the x-axis and z-axis is not significant. In addition, the high-frequency signal in the x-axis is mainly the quintuple frequency area, while the spectrum signal in the y direction is relatively scattered, mainly concentrated in the double frequency area and quintuple frequency area. The spectrum signal in the z-axis is mainly concentrated in the

frequency doubling area. The results indicate that under the working condition of 18 Hz, the spectral characteristics in x-axis, y-axis and z-axis are all in line with the ideal operating conditions, and the pump operates in a good status.

Table 9. The range of critical operating condition obtained from vibration at different positions.

Vibration at Different Positions	Range of Critical Operating Condition
Vibration of the pump	[30 Hz, 35 Hz]
Motor vibration	[15 Hz, 20 Hz]
Shaft vibration	[30 Hz, 35 Hz]
	[15 Hz, 20 Hz]
	[30 Hz, 35 Hz]

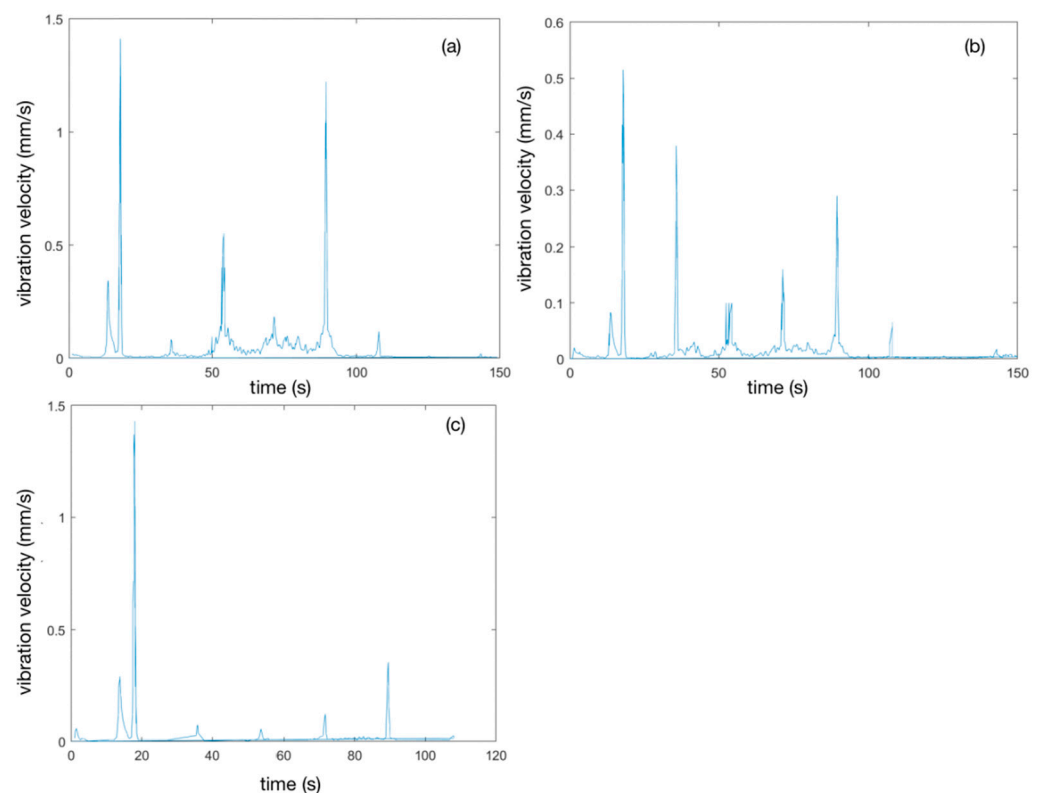


Figure 7. Spectrum diagram of the vibration signals of the monitoring point at the top of the motor in (a) x-axis, (b) y-axis and (c) z-axis under the working condition of 18 Hz.

Figure 8 illustrates energy extraction diagram of the shaft vibration signal obtained from the wavelet transform under the working condition of 18 Hz. The wavelet analysis is used to identify the characteristics of vibration energy distribution over time. As shown in Figure 8, under the operating condition of 18 Hz, the vibration energy in the x-axis mainly occurs at 0.6 s and 0.85 s, while the vibration energy in the y-axis direction mainly occurs at 0.03 s and 0.2 s.

Figure 9 shows the spectrum diagram of the vibration signals of the monitoring point at the top of the motor under the working condition of 33 Hz. In the spectrum of the x-axis, vibration is mainly concentrated in the quintuple frequency area and frequency doubling area with significant high-frequency signals. In the spectrum of the y-axis, high-frequency vibrations outside the quintuple frequency are obvious. In the spectrum of the z-axis, vibrations are concentrated on the frequency with significant high-frequency signals. The results indicate that the vibration state of the motor deviates from normal status when the pump works under the operating condition of 33 Hz, which limits the performance of the

water pump. Long-term operating of the pump under this working condition may lead to damage to the equipment.

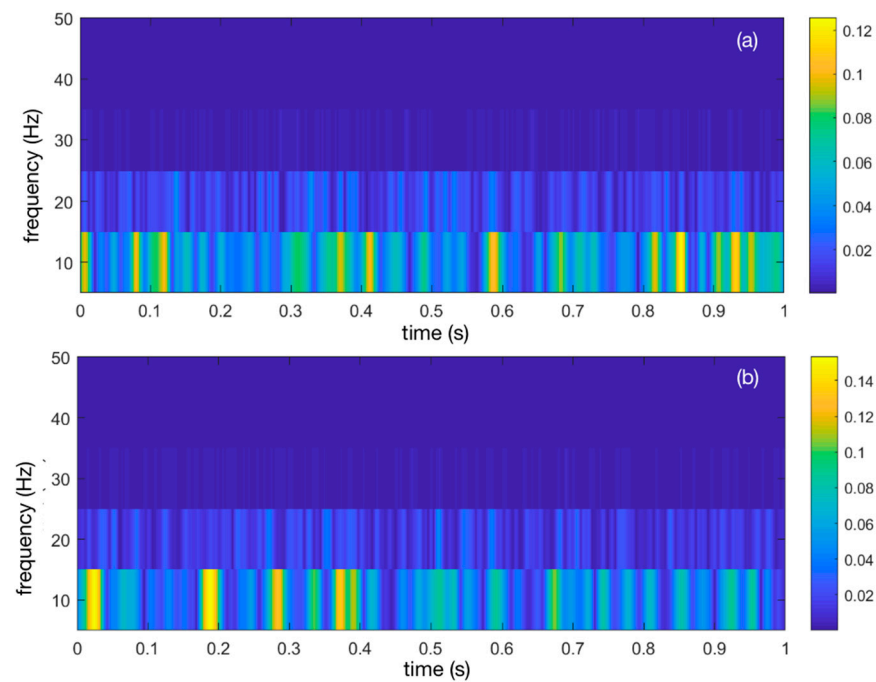


Figure 8. Energy extraction of shaft vibration signal using wavelet analysis in (a) x-axis and (b) y-axis under the working condition of 18 Hz.

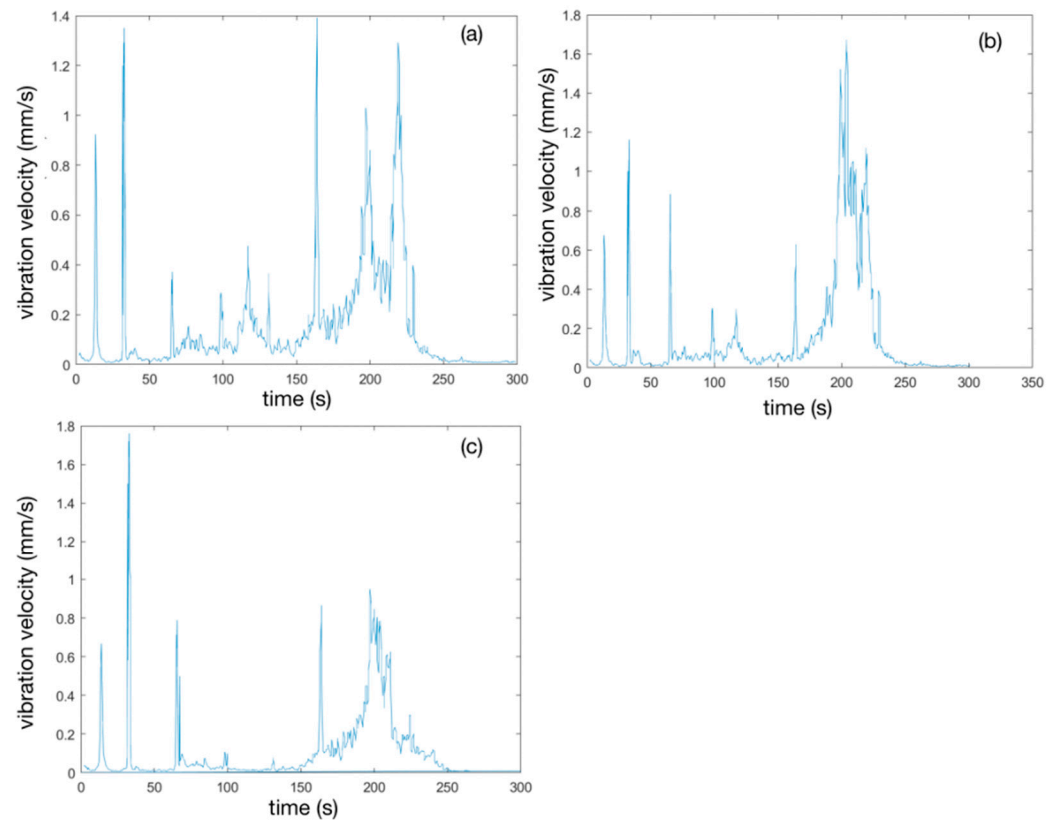


Figure 9. Spectrum diagram of the vibration signals of the monitoring point at the top of the motor in (a) x-axis, (b) y-axis and (c) z-axis under the working condition of 33 Hz.

Figure 10 illustrates the energy extraction diagram of the shaft vibration signal obtained from the wavelet transform under the working condition of 33 Hz. Under the operating condition of 33 Hz, the vibration energy in the x-axis mainly occurs at 0.59 s, 0.88 s and 0.91 s, while the vibration energy in the y-axis mainly occurs at 0.52 s, 0.73 s and 0.91 s.

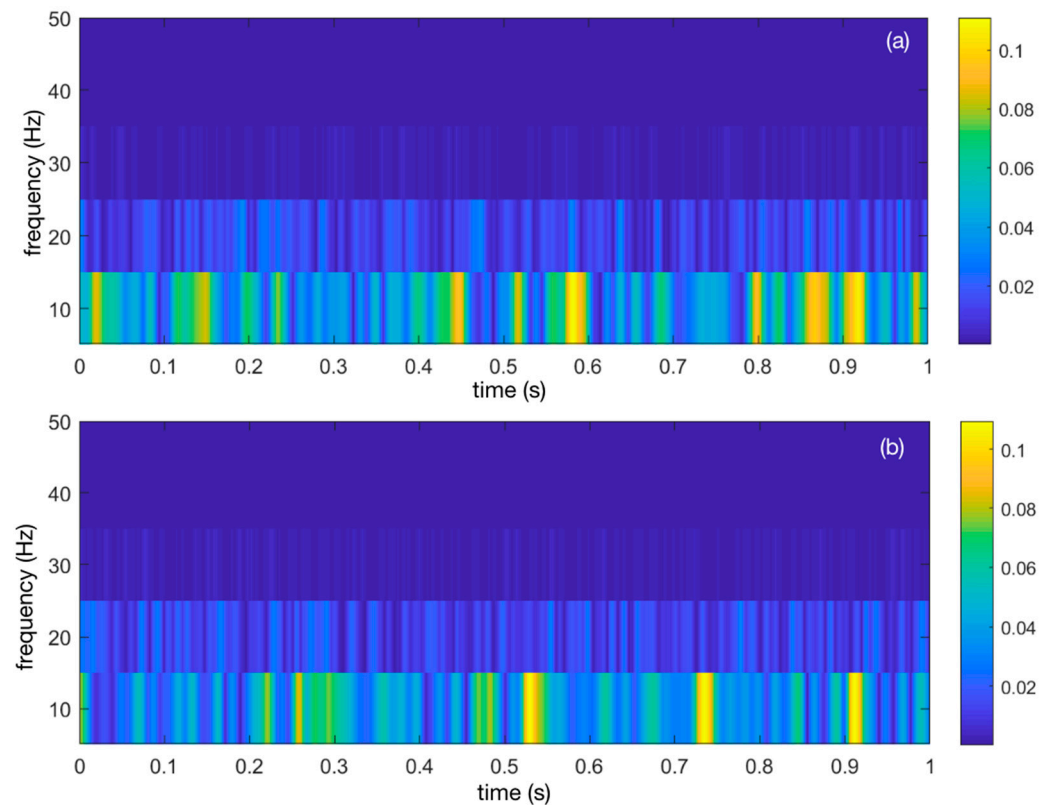


Figure 10. Energy extraction of shaft vibration signal using wavelet analysis in (a) x-axis and (b) y-axis under the working condition of 33 Hz.

By analyzing the frequency spectrum of the monitoring points at the top of the motor of the vertical centrifugal variable frequency water pump under the operating conditions of 18 Hz and 33 Hz, we can see that the working status of 18 Hz operating condition is good, while high-frequency and large vibration signals appear at the frequency spectrum of the 33 Hz operating condition. This indicates that the operating status of the pump has deteriorated under the operating condition of 33 Hz. The specific motor vibration under these two operating conditions are shown in Table 10. Based on the data exhibited in Tables 4 and 10, within the operating range of [15 Hz, 20 Hz], the difference in vibration values between the 18 Hz operating condition and the 15 Hz operating condition is mainly concentrated in the frequency doubling, with a difference of 0.2 mm/s in the x-axis, 3.2 mm/s in the y-axis and 4 mm/s in the z-axis. However, the difference in vibration values between the 18 Hz operating condition and the 20 Hz operating condition is not significant. Within the operating range of [30 Hz, 35 Hz], the difference in vibration values between 35 Hz and 30 Hz is mainly the x-axis and z-axis of the double frequency area as well as the x-axis of quadruple frequency area. Comparing the vibration value of 33 Hz operating conditions with 35 Hz and 30 Hz conditions, it can be found that its vibration is exactly between 30 Hz and 35 Hz and is higher than 30 Hz. Based on the above analysis, it can be determined that the critical operating condition within the operating range of [15 Hz, 20 Hz] is 16 Hz or 17 Hz. As the vibration values between 18 Hz and 20 Hz operating conditions are similar, the critical operating condition should take the lower value, i.e., 16 Hz. Within the operating range of [30 Hz, 35 Hz], the critical operating condition is 33 Hz.

Table 10. Motor vibration under different operating conditions.

Test Conditions	Revolution Speed (r/min)	Frequency Doubling (mm/s)	Double Frequency (mm/s)	Triple Frequency (mm/s)	Quadruple Frequency (mm/s)	Quintuple Frequency (mm/s)
18 Hz (X)	1044	1.4124	0.0869	0.5517	0.1883	1.2239
18 Hz (Y)		0.5142	0.3778	0.0928	0.1601	0.2906
18 Hz (Z)		1.4349	0.0747	0.0573	0.1439	0.3542
33 Hz (X)	1914	1.3477	0.3712	0.295	0.3676	1.388
33 Hz (Y)		1.1606	0.8835	0.305	0.052	0.6333
33 Hz (Z)		1.7616	0.788	0.1053	0.0834	0.8678

5.2. Fault Diagnosis of Variable Frequency Pump

Based on the standard <<Vibration measurement and evaluation methods of pumps>> GBT29531-2013 and the vibration data under the working conditions of 15 Hz, 18 Hz, 20 Hz, 25 Hz, 30 Hz, 33 Hz, 35 Hz, 40 Hz, 45 Hz and 50 Hz, the vibration levels are classified into four different levels: A, B, C and D (Table 11). Level A means the health status of the pump is 'normal', level B means the health status of the pump is 'abnormal' and level C and D mean the health status of the pump is 'fault'.

Table 11. Level of vibration and health status of variable frequency pump.

Test Conditions	Pump Vibration Level	Motor Vibration Level	Synthetic Vibration Level	Health Status of the Pump
15 Hz	A	D	D	fault
18 Hz		A	A	normal
20 Hz	A	B	B	abnormal
25 Hz	A	A	A	normal
30 Hz	A	A	A	normal
33 Hz		B	B	abnormal
35 Hz	B	B	B	abnormal
40 Hz	B	C	C	fault
45 Hz	B	C	C	fault
50 Hz	B	D	D	fault

The health status evaluation of the variable frequency water pump is mainly based on the determination of critical operating conditions and the classification of health status levels of the pump. The health status of the variable frequency water pump is divided into four operating ranges at 0 to 50 Hz (see Table 12). Then, the performance of the variable frequency water pump can be evaluated according to the flow rate-efficiency characteristic curve indicated in Figure 11.

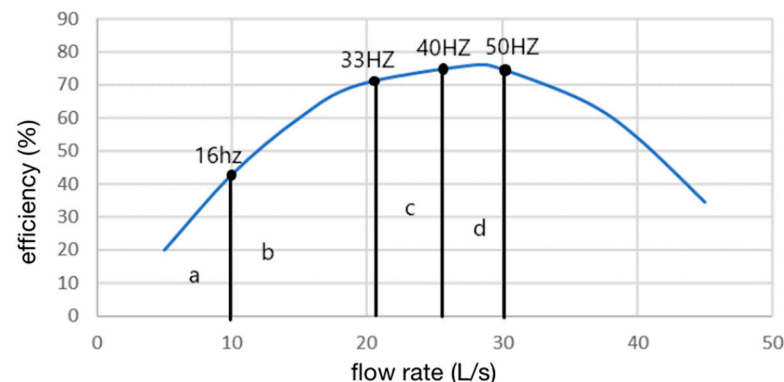
**Figure 11.** The characteristic curve of variable frequency water pump.

Table 12. The health status of water pump under different operating conditions.

Test Conditions	0–16 Hz	16–33 Hz	33–40 Hz	40–50 Hz
status	fault	normal	abnormal	fault

As shown in Figure 11, the characteristic curve of the variable frequency water pump is divided into four intervals: a, b, c and d. Among which, interval a corresponds to the 0–17 Hz operating range, interval b corresponds to the 17–33 Hz operating range, interval c corresponds to the 33–40 Hz operating range and interval d corresponds to the 40–50 Hz operating range. According to the efficiency curves at different intervals, it can be seen that the efficiency of the pump in interval a is the lowest, the efficiency of the pump in interval b shows a continuous increasing tendency, the efficiency of the pump in interval c remains stable around the maximum value and the pump efficiency reached its maximum value in interval d.

In summary, the principle recommended operating range for a variable frequency water pump is [16 Hz, 33 Hz], i.e., interval b. As the efficiency of the water pump in this interval is high, the operating conditions of the water pump can be flexibly adjusted according to the actual needs of the water transmission process, and the operating performance is the best within this range. The second recommended operating range is [33 Hz, 40 Hz], i.e., interval c. This is because the efficiency of the variable frequency water pump within this operating range is the highest, but the adjustable efficiency range is very small, which means this operating range is suitable for scenarios with high water delivery flow requirements. The operating range of [0 Hz, 16 Hz], i.e., interval a, should be avoided. In this range, the vibration of the pump unit is harsh and the operating efficiency is low, making it prone to major faults and affecting the stable operation of the pump. Similarly, the pump should also be avoided from operating within the operating range of [40 Hz, 50 Hz], i.e., interval d. As the efficiency of the pump reaches its maximum within this operating range, the upstream reservoir water level exceeds the warning level or emergency flood controls are required; short-term operation within this operating range can be considered.

6. Conclusions

The monitoring and analysis of the operation performance of variable-frequency pumps can provide a basis for fault diagnosis, which is related to the safety of water supply systems. According to the structural characteristics of a vertical centrifugal variable-frequency pump, six monitoring points were selected and different types of sensors were arranged to collect signals. Through a comprehensive analysis of the signals acquired by multiple sensors, the accuracy of the operation performance analysis and fault diagnosis was improved. The signals were preprocessed via smoothing, waveform trend adjustment and filtering to eliminate the high-frequency noise signals, and to prevent the overall waveform from deviating from the reference line. The frequency spectrum features of the vibration velocity and vibration acceleration signals collected at the measuring points were extracted. In order to simplify the chaotic periodic components and improve the accuracy of the spectrum analysis of nonstationary signals, the cepstrum analysis method was used. The vibration displacement signal was processed using the power spectrum estimation method, and the influence of the interference signal was avoided through statistical characteristic analysis.

The results of fault diagnosis indicate that the principle recommended operating range for a variable frequency water pump is [16 Hz, 33 Hz]; as the efficiency of the water pump in this interval is high, the operating conditions of the water pump can be flexibly adjusted according to the actual needs of the water transmission process, and the operating performance is the best within this range. The second recommended operating range is [33 Hz, 40 Hz], as the efficiency of the variable frequency water pump within this operating range is the highest, but the adjustable efficiency range is very small. In addition,

it should be avoided that the pump operates within the operating range of [0 Hz, 16 Hz] and [40 Hz, 50 Hz].

Author Contributions: Conceptualization, J.H., C.W. and C.S.; methodology, J.H.; writing—original draft, J.H.; writing—review and editing, J.H., Y.G. and C.W. All authors have read and agreed to the published version of the manuscript.

Funding: This work is supported by the Joint Funds of the Zhejiang Provincial Natural Science Foundation of China (LZJWZ22E090004).

Data Availability Statement: Data available upon request.

Acknowledgments: We are very grateful to anonymous reviewers for their constructive comments and suggestions.

Conflicts of Interest: The authors declare no conflict of interest.

References

1. Shi, Z.; Xu, Y.; Li, Y. Wavelet-based Synchroextracting Transform: An effective TFA tool for machinery fault diagnosis. *Control Eng. Pract.* **2021**, *114*, 104884. [[CrossRef](#)]
2. Xue, Z.; Cao, X.; Wang, T. Vibration test and analysis of centrifugal pump. *J. Irrig. Drain. Mach. Eng.* **2018**, *36*, 466–471.
3. Xue, Z. Analysis and Solution of Vibration Failures Diagnosis for the Multistage Centrifugal Pumps. *Noise Vib. Control* **2018**, *38*, 225–228. [[CrossRef](#)]
4. Liu, T.; Li, J.; Cai, X. A time-frequency analysis algorithm for ultrasonic waves generating from a debonding defect by using empirical wavelet transform. *Appl. Acoust.* **2018**, *131*, 16–27. [[CrossRef](#)]
5. Saimurugan, M.; Ramprasad, R. A dual sensor signal fusion approach for detection of faults in rotating machines. *J. Vib. Control* **2018**, *24*, 2621–2630. [[CrossRef](#)]
6. Ghosh, N.; Saha, S.; Paul, R. IDCR: Improved Dempster Combination Rule for multisensor fault diagnosis. *Eng. Appl. Artif. Intell.* **2021**, *104*, 104369. [[CrossRef](#)]
7. Liu, J.; Zheng, J.; Zhang, W. Instantaneous frequency identification of signals based on improved synchrosqueezing wavelet transform. *J. Vib. Meas. Diagn.* **2017**, *37*, 814–821.
8. An, X.; Yang, W. Vibration signal analysis of a hydropower unit based on adaptive local iterative filtering. Proceedings of the Institution of Mechanical Engineers. *J. Mech. Eng. Sci.* **2017**, *231*, 1339–1353. [[CrossRef](#)]
9. Zhang, D.; Feng, Z. Enhancement of time-frequency post-processing readability for nonstationary signal analysis of rotating machinery: Principle and validation. *Mech. Syst. Signal Proc.* **2022**, *163*, 108145. [[CrossRef](#)]
10. Ahmad, Z.; Rai, A.; Maliuk, A.; Kim, J. Discriminant Feature Extraction for Centrifugal Pump Fault Diagnosis. *IEEE Access* **2020**, *8*, 165512–165528. [[CrossRef](#)]
11. Shen, J.; Pan, T.; Mao, X.; Wu, T.; Gu, F. Study on Condition Detection of Major Equipment in Nuclear Power Plants Based on Fuzzy Synthetic Assessment. *Nucl. Power. Eng.* **2018**, *39*, 104–110. [[CrossRef](#)]
12. Lei, Y.; Fan, W.; Li, Z.; Liang, Y.; Fang, M.; Wang, J. A Fault Diagnosis Model for Rotating Machinery Using VWC and MSFLA-SVM Based on Vibration Signal Analysis. *Shock Vib.* **2019**, *2019*, 1908485. [[CrossRef](#)]
13. Moosavian, A.; Khazaei, M.; Ahmadi, H.; Khazaei, M.; Najafi, G. Fault diagnosis and classification of pump using adaptive neuro-fuzzy inference system based on vibration signals. *Struct. Health Monit.* **2015**, *14*, 402–410. [[CrossRef](#)]
14. Jia, Y.; Xu, M.; Wang, R. Symbolic Important Point Perceptually and Hidden Markov Model Based Hydraulic Pump Fault Diagnosis Method. *Sensors* **2018**, *18*, 4460. [[CrossRef](#)]
15. Strömbergsson, D.; Marklund, P.; Berglund, K. Increasing Wind Turbine Drivetrain Bearing Vibration Monitoring Detectability Using an Artificial Neural Network Implementation. *Appl. Sci.* **2021**, *11*, 3588. [[CrossRef](#)]
16. Jiang, W.; Wang, C.; Zou, J.; Zhang, S. Application of Deep Learning in Fault Diagnosis of Rotating Machinery. *Processes* **2021**, *9*, 919. [[CrossRef](#)]
17. Zhang, M.; Jiang, Z.; Feng, K. Research on variational mode decomposition in rolling bearings fault diagnosis of the multistage centrifugal pump. *Mech. Syst. Signal Proc.* **2017**, *93*, 460–493. [[CrossRef](#)]
18. Michael, S.; John, T. An Industrial Digitalization Platform for Condition Monitoring and Predictive Maintenance of Pumping Equipment. *Sensors* **2019**, *19*, 3781. [[CrossRef](#)]
19. Panda, A.; Rapur, J.; Tiwari, R. Prediction of flow blockages and impending cavitation in centrifugal pumps using Support Vector Machine (SVM) algorithms based on vibration measurements. *Measurement* **2018**, *130*, 44–56. [[CrossRef](#)]
20. Irfan, M.; Alwadi, A.; Glowacz, A.; Awais, M.; Rahman, S.; Khan, M.; Jalalah, M.; Alshorman, O.; Caesarendra, W. A Novel Feature Extraction and Fault Detection Technique for the Intelligent Fault Identification of Pump Bearings. *Sensors* **2011**, *21*, 4225. [[CrossRef](#)]
21. Wang, Y.; Liu, N.; Guo, H.; Wang, X. An engine-fault-diagnosis system based on sound intensity analysis and wavelet packet pre-processing neural network. *Eng. Appl. Artif. Intell.* **2020**, *94*, 103765. [[CrossRef](#)]

22. Zhu, Y.; Li, G.; Wang, R.; Tang, S.; Su, H.; Cao, K. Intelligent Fault Diagnosis of Hydraulic Piston Pump Based on Wavelet Analysis and Improved AlexNet. *Sensors* **2021**, *21*, 549. [[CrossRef](#)] [[PubMed](#)]
23. Thelaidjia, T.; Chenikher, S.; Moussaoui, A. Optimal wavelet analysis and enhanced independent component analysis for isolated and combined mechanical faults diagnosis. *Int. J. Adv. Mech. Syst.* **2020**, *8*, 116–126. [[CrossRef](#)]
24. Li, Z.; Jiang, W.; Zhang, S.; Sun, Y.; Zhang, S. A Hydraulic Pump Fault Diagnosis Method Based on the Modified Ensemble Empirical Mode Decomposition and Wavelet Kernel Extreme Learning Machine Methods. *Sensors* **2021**, *21*, 2599. [[CrossRef](#)]
25. Xie, Y.; Yan, Y.; Li, G.; Li, X. Scintillation detector fault diagnosis based on wavelet packet analysis and multi-classification support vector machine. *J. Instrum.* **2020**, *15*, 3001. [[CrossRef](#)]
26. He, R.; Xu, P.; Chen, Z.; Luo, W.; Su, Z.; Mao, J. A non-intrusive approach for fault detection and diagnosis of water distribution systems based on image sensors, audio sensors and an inspection robot. *Energy Build.* **2021**, *243*, 110967. [[CrossRef](#)]
27. Deng, S.; Pei, J.; Wang, Y.; Liu, B. Research on drilling mud pump fault diagnosis based on fusion of acoustic emission and vibration technology. *Insight* **2017**, *59*, 415–423. [[CrossRef](#)]

Disclaimer/Publisher's Note: The statements, opinions and data contained in all publications are solely those of the individual author(s) and contributor(s) and not of MDPI and/or the editor(s). MDPI and/or the editor(s) disclaim responsibility for any injury to people or property resulting from any ideas, methods, instructions or products referred to in the content.